Supplementary Information

Incorporation of tetrahedral ferric iron in single crystals of hydrous ringwoodite

A.R. Thomson[1,2*], R. Piltz[3], W. Crichton[2], V. Cerentola[3,4], I.S. Ezad[1,5], D.P. Dobson[1,6], I.G. Wood[1] and J. Brodholt[1,7]

[1]*Department of Earth Sciences, University College London, London, WC1E 6BT.*
[2]*ESRF- The European Synchrotron, 38043 Grenoble, France*
[3]*Bragg Institute, Australian Nuclear Science and Technology Organisation, Australia.*
[4]*European X-ray free-electron laser, Hamburg, Germany*
[5]*Department of Earth and Environmental Sciences, Macquarie University. Australia*
[6]*Bayeriches Geoinstitut, University of Bayreuth, 95440 Bayreuth, Germany.*
[7]*Centre for Earth Evolution and Dynamics, University of Oslo, N-0316 Oslo, Norway*
*Corresponding Author (a.r.thomson@ucl.ac.uk)

In addition to the hydrous ringwoodite crystals studied and reported throughout the main text, work in this study also included synthesis of a second iron bearing ringwoodite sample under water-free conditions. Experimental synthesis conditions were achieved using an 8/3 multi-anvil assembly with a TiB_2:BN furnace at ~ 21 GPa and 1400 °C. The run products were observed to be fine grained, were pale green in colour and mostly composed of ringwoodite. As the synthetic crystals were too small for single-crystal studies, the run products were analysed using X-ray powder diffraction (λ = 0.2296 Å) and observed to consist of a mixture of ringwoodite and ferropericlase (Supplementary figure 1a). FTIR spectroscopy confirmed the sample was water-poor and SMS reveals clear doublets for octahedral ferrous iron in ringwoodite (CS=1.03, QS=2.72) and ferropericlase (CS=1.04, QS=0.57), alongside a weak ferric iron signal (Supplementary figure 1b and c). Whilst the origin of this weak signal isn't completely certain, as it can be equally well explained by octahedral ferric iron in ringwoodite (CS=0.6, QS=0.95, similar to McCammon et al. 2004) or ferric iron in ferropericlase (CS=0.25, QS=0, similar to McCammon et al. 1998), it cannot be explained by tetrahedral ferric iron in either ringwoodite or ferropericlase.

Supplementary Table 1: Results of the X-ray and neutron single-crystal refinements

XRD (300 K)	**Mg^A**	±	**Fe^A**	±	**Si^A**	±	**Si^B**	±	**Fe^B**	±	**O**	±	**A_{tot}**	**B_{tot}**
occupancy	**1.728**	-	**0.133**	*0.001*	**0.123**	*0.002*	**0.885**	*0.002*	**0.045**	*0.001*	**4.000**		1.99	0.93
U_{iso}	0.0059	*0.0001*	0.0059	*0.0001*	0.0059	*0.0001*	0.0042	*0.0002*	0.0042	*0.0002*	0.0059	*0.0001*	**GOF(obs)**	**r(obs)**
									x, y, z		0.2435	*0.0000*	1.43	0.98

Neutron (300 K)	**Mg^A**	±	**Fe^A**	±	**Si^A**	±	**Si^B**	±	**Fe^B**	±	**O**	±	**Atot**	**Btot**
occupancy	**1.728**	-	**0.156**	*0.006*	**0.085**	*0.014*	**0.923**	*0.014*	**0.023**	*0.006*	**4.000**	-	1.97	0.95
U_{iso}	0.0066	*0.0013*	0.0066	*0.0013*	0.0066	*0.0013*	0.0045	*0.0012*	0.0045	*0.0012*	0.0065	*0.0006*	**GOF(obs)**	**r(obs)**
									x, y, z		0.2437	*0.0002*	1.95	4.12

Neutron (300 K)	**Mg^A**	±	**Fe^A**	±	**Si^A**	±	**Si^B**	±	**Fe^B**	±	**O**	±	**H^A**	±	**Atot**	**Btot**
occupancy	**1.728**	-	**0.159**	*0.004*	**0.085**	*0.010*	**0.923**	*0.010*	**0.020**	*0.004*	**4.000**	-	**0.244**	*0.062*	2.22	0.94
U_{iso}	0.0072	*0.0089*	0.0072	*0.0089*	0.0072	*0.0089*	0.0069	*0.0089*	0.0069	*0.0089*	0.0069	*0.0089*	0.0015	*0.0129*	**GOF(obs)**	**r(obs)**
										x	0.2437	*0.0001*	0.5073	*0.0060*	1.49	3.33
										y	0.2437	*0.0001*	0.1862	*0.0062*		
										z	0.2437	*0.0001*	0.3942	*0.0078*	**wt.% H_2O**	2.19

Neutron (100 K)	**Mg^A**	±	**Fe^A**	±	**Si^A**	±	**Si^B**	±	**Fe^B**	±	**O**	±	**Atot**	**Btot**
occupancy	**1.728**	-	**0.129**	*0.005*	**0.085**	*0.012*	**0.922**	*0.012*	**0.050**	*0.005*	**4.000**	-	1.94	0.97
U_{iso}	0.0051	*0.0002*	0.0053	*0.0002*	0.0053	*0.0002*	0.0062	*0.0006*	0.0061	*0.0006*	0.0056	*0.0005*	**GOF(obs)**	**r(obs)**
									x, y, z		0.2437	*0.0001*	1.11	3.26

Neutron (100K)	**Mg^A**	±	**Fe^A**	±	**Si^A**	±	**Si^B**	±	**Fe^B**	±	**O**	±	**H^A**	±	**H^B**	±	**A_{tot}**	**B_{tot}**
occupancy	**1.728**	-	**0.130**	*0.002*	**0.082**	*0.005*	**0.926**	*0.005*	**0.049**	*0.002*	**4.000**	-	**0.072**	*0.077*	**0.114**	*0.022*	2.01	1.09
U_{iso}	0.0131	*0.0003*	0.0131	*0.0003*	0.0131	*0.0003*	0.0143	*0.0003*	0.0143	*0.0003*	0.0132	*0.0337*	0.3206	*0.0560*	0.0742	*0.0327*	**GOF(obs)**	**r(obs)**
										x	0.2438	*0.0001*	0.0844	*0.0578*	0.0421	*0.0116*	1.03	3.07
										y	0.2438	*0.0001*	0.3684	*0.0575*	0.1250	-		
										z	0.2438	*0.0001*	0.0161	*0.0793*	0.1250	-	**wt.% H_2O**	1.16

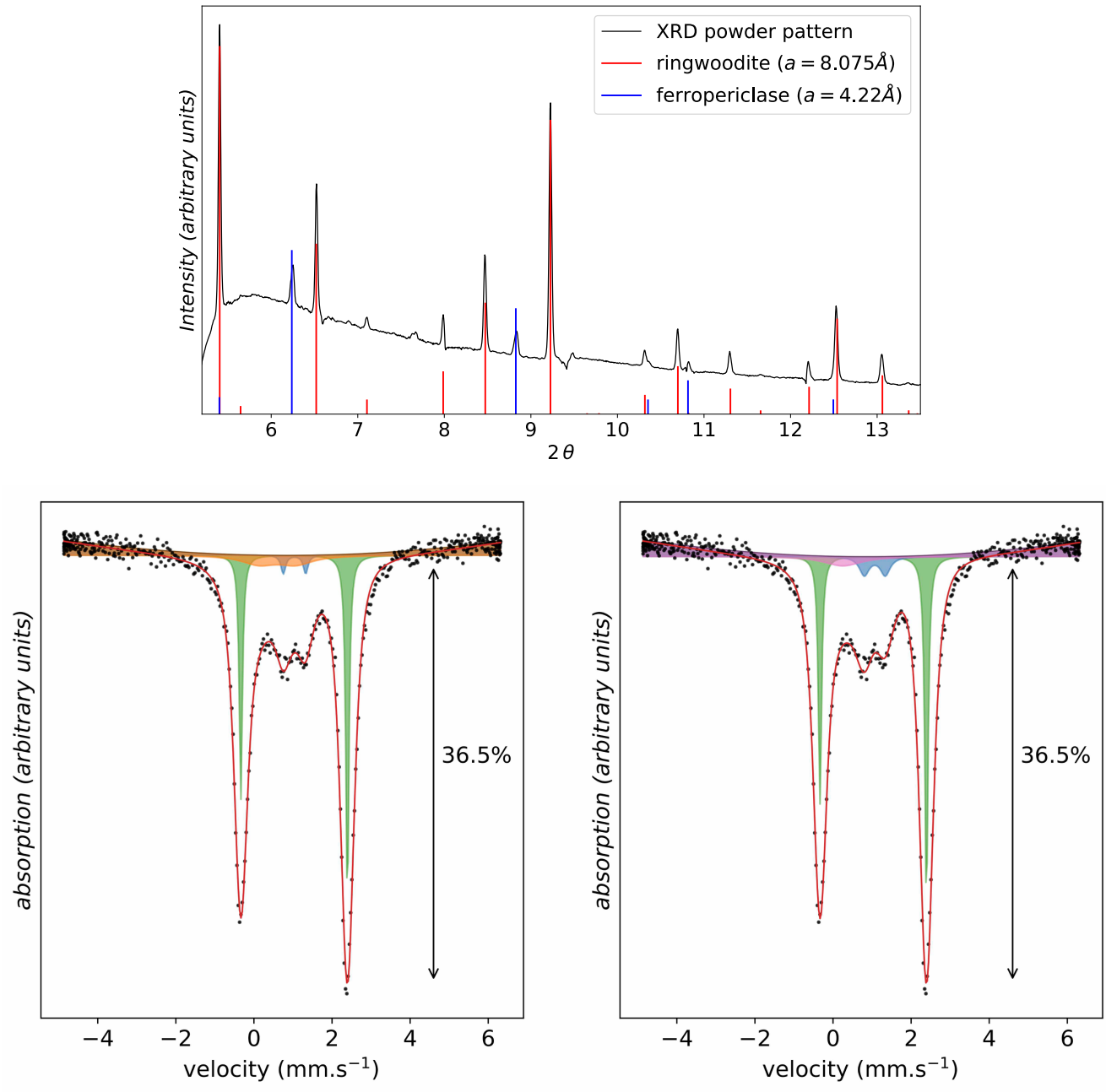

Supplementary Figure 1: (a) diffraction pattern of water-poor, pale green-coloured polycrystalline ringwoodite sample, confirming it is composed of a mixture of ringwoodite and ferropericlase. (b) and (c) SMS spectra collected from water-poor polycrystalline green-coloured ringwoodite sample, fitted using two models using MossA (Prescher et al. 2012). (b) and (c) are both fitted with two components corresponding to octahedral ferrous iron in ringwoodite (green) and ferropericlase (blue), whilst the third additional component is consistent with (b) octahedral ferric iron in ringwoodite (orange) or (c) ferric iron in ferropericlase (pink).

References

McCammon, C.A., Frost, D.J., Smyth, J.R., Laustsen, H.M.S., Kawamoto, T., Ross, N.L., and van Aken, P.A. (2004) Oxidation state of iron in hydrous mantle phases: Implications for subduction and mantle oxygen fugacity. Physics of the Earth and Planetary Interiors, 143, 157–169.

McCammon, C., Peyronneau, J., and Poirier, J.-P. (1998) Low ferric iron content of (Mg,Fe)O at high pressures and temperatures. Geophysical Research Letters, 25, 1589–1592.

Prescher, C., McCammon, C., and Dubrovinsky, L. (2012) MossA: a program for analyzing energy-domain Mössbauer spectra from conventional and synchrotron sources. Journal of Applied Crystallography, 45, 329–331.